Polarity effect for exploding wires in a vacuum

G. S. Sarkisov,* P. V. Sasorov,† K. W. Struve, D. H. McDaniel, A. N. Gribov,‡ and G. M. Oleinik‡
Sandia National Laboratories, Albuquerque, New Mexico 87185
(Received 17 April 2002; published 21 October 2002)

Experimental evidence for a strong influence of the radial electric field on energy deposition into thin metal wires during their electrical explosion in vacuum is presented. Explosion of the metal wire with a positive polarity when the radial electric field ''pushes'' electrons into the wire results in twice as much deposited energy than with the negative polarity when the radial field ''expels'' electrons from the wires. Moreover, the axial structure of the deposited energy changes. This effect can be explained by the influence of radial electric field on electronic emission and on vapor breakdown along the wire surface.

DOI: 10.1103/PhysRevE.66.046413 PACS number(s): 52.80.Qj, 51.50.+v

Investigation of the initial stage of an exploding wire is very important for modern *Z*-pinch physics. Impressive results have recently been achieved on the high-current *Z* accelerator at Sandia National Laboratories using multiwire array loads [1,2]. It has been recognized that symmetry and parameters of the initial plasma shell play an important role for stability of the final stagnation and the x-ray yield. Direct influence of the current prepulse on the x ray yields for an Al wire array load on 1-MA installation was demonstrated in Ref. [3].

Fast electrical heating of a metal wire in vacuum terminates with vapor breakdown along the vacuum-wire interface when a low-resistance plasma shell is formed, which results in a voltage and energy-deposition collapse [4,5]. It is assumed [4] that surface impurities, such as absorbed gases and hydrocarbons, play an important role in termination of energy deposition processes. The assumption is that the heated fast-vaporizing impurities create a gas shell around the wire and that after field breakdown the current is switched from the wire to the ionized gas shell [6]. It has been shown [4,5] that the explosion of wires in a high-density medium results in enhanced energy deposition. Recent investigations [7] demonstrate enhanced energy deposition for wires with a dielectric coating. Earlier surface breakdown leads to lower energy deposition into the wire. It has been noted in Refs. [5], [8], [9] that with a higher rate of current rise more energy is deposited before surface breakdown. Explosion of the W wire with a slow current rate ~20 A/ns results in wire disintegration on a macroscale [9] due to surface breakdown before melting, which is initiated by anomalously high electron emission [5]. With a higher current rise ~150 A/ns, the wire passes through an ''energy deposition barrier'' for W and vaporizes/microdisintegrates before surface breakdown [9]. In this paper, we present experimental evidence for strong influence of the radial electric field on the value and structure of energy deposition into the wire, and its dependence on the density of the surrounding medium.

A 100-kV Maxwell 40151-B pulse generator with a 7-nF capacitor bank, with a charging voltage of 60 kV and a stored energy of 12.6 J, provides the electrical pulse to drive the wire explosions. The pulser can operate in positive (initially) and negative (after adaptation) polarity modes. Thin, 20-μm-diameter, 20-mm-long metallic wires were centered in a coaxial reverse current cap that contained four diagnostic windows. It was located in a vacuum chamber evacuated to a pressure of $\sim 10^{-4}$–10^{-5} Torr to prevent gas breakdown. A 9-m-long 50 Ω coaxial cable delivered the electrical pulse from the generator to the wire. A diagram of the vacuum chamber with a coaxial target unit is shown in Fig. 1.

The experimental setup functions in the fast rise-time mode with a current rate of 150 A/ns into a short circuit (~3-kA maximum), and a voltage rate of 12 kV/ns in an open circuit (~120-kV maximum). The downstream current through the wire was measured with a 2-GHz bandwidth, 0.1-Ω coaxial-shunt resistor. The anode-ground voltage was

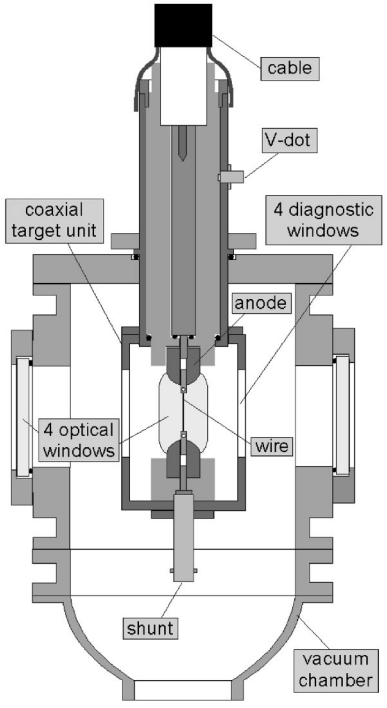

FIG. 1. Vacuum chamber with coaxial target unit.

*Ktech Corporation, Albuquerque, NM 87106. Email address: gssarki@sandia.gov
†Institute of Theoretical and Experimental Physics, Moscow, 117259, Russia.
‡SSC RF TRINITI, 142190 Troitsk, Moscow Region, Russia.

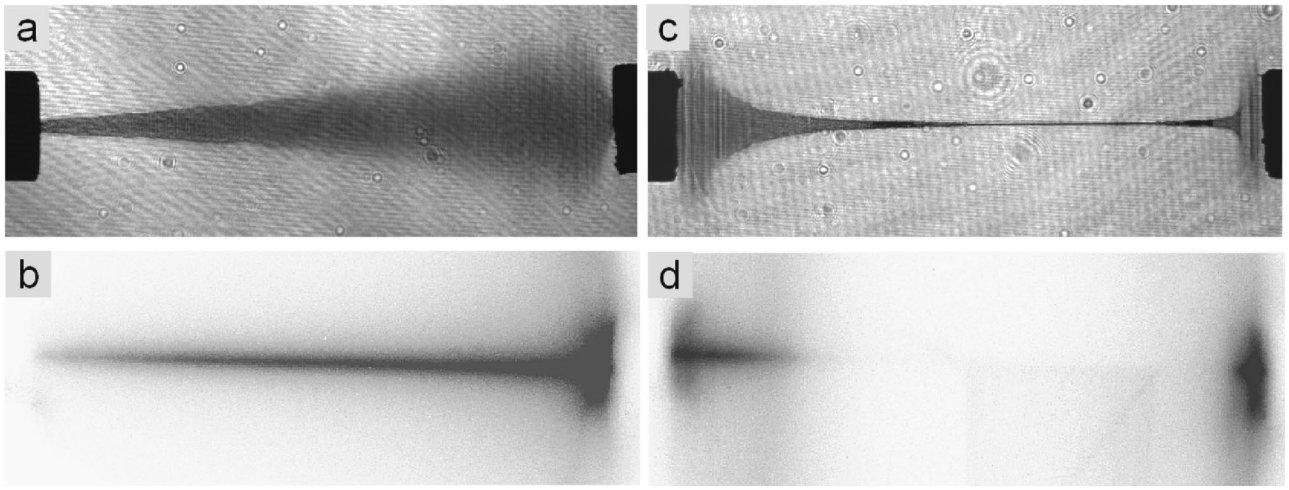

FIG. 2. Laser shadowgrams at 1 μs after voltage maximum (a),(c) and time-integrated open-shutter images (b),(d) of a fast-exploding 20-μm Ti wire with a positive (a),(b) and negative (c),(d) polarity pulse. The anode is on the right for (a),(b) and on the left for (c),(d).

measured with a V dot (capacitive divider for measurement of dV/dt). A Si PIN-diode with a 1-ns rise time monitored the power of light emission from the exploding wire. Open-shutter time-integrated charge-coupled device images of the exploding wire allow monitoring the two-dimensional structure of the deposited energy in a visible light wavelength. A stimulated Brillouin scattering (SBS)-compressed Nd:YAG (yttrium aluminum garnet) *Q*-switch laser (EKSPLA SL 312) with 120 mJ of energy at 532 nm and with a 150-ps pulse duration was used for shadowgraphy of the exploding wire. All electrical wave forms were captured with a four-channel 1-GHz digital scope, Tektronix TDS 684C.

Figure 2 shows laser shadowgrams at 1 μs after voltage maximum [Figs. 2(a), 2(c)] and complementary open-shutter images [Figs. 2(b), 2(d)] of fast exploding 20-μm-diameter and 2-cm-long Ti wires with positive [Figs. 2(a), 2(b)] and negative [Figs. 2(c), 2(d)] polarities. In the positive-polarity explosion, we see a conical structure of the deposited energy, which grows from cathode to anode [Fig. 2(a)]. In the negative-polarity explosion, we see enhanced energy deposition near the anode and cathode, and very poor deposition in the central part of the wire [Fig. 2(c)]. The open-shutter images demonstrate the same energy deposition as the corresponding laser shadowgrams. The current, voltage, and light emission wave forms for positive- and negative-polarity explosions are presented in Figs. 3(a) and 3(b). The maximum

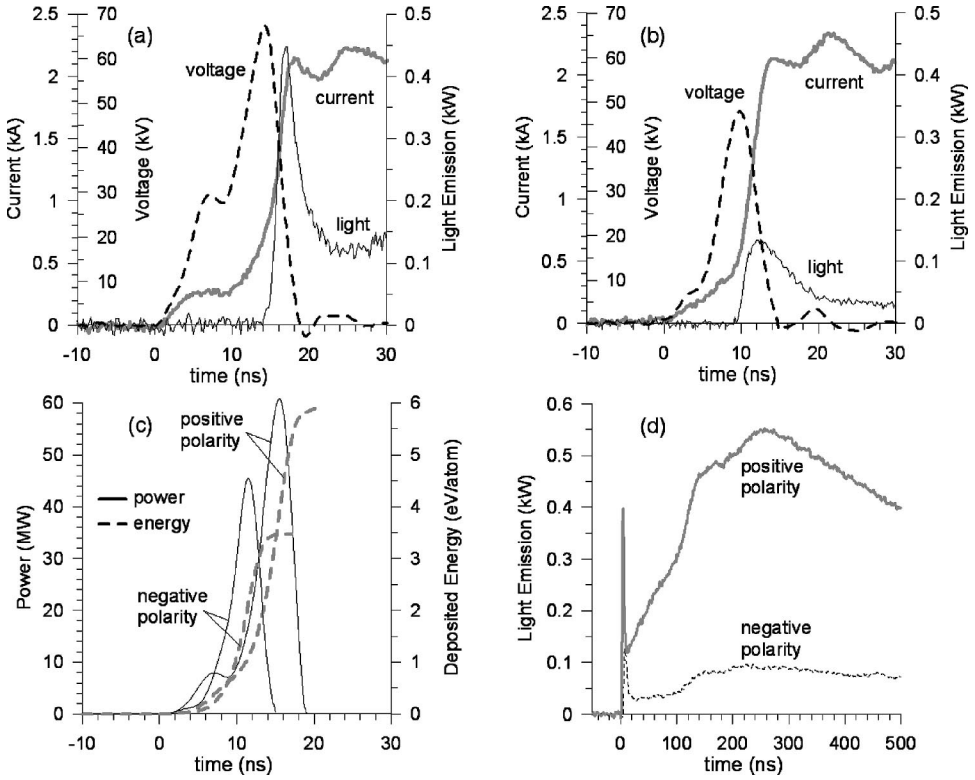

FIG. 3. Current, voltage, and light emission wave forms for explosion in vacuum of 20-μm Ti wires with positive (a) and negative (b) polarity. The evolution of electrical power and deposited energy (c), and large time-scale light emission (d).

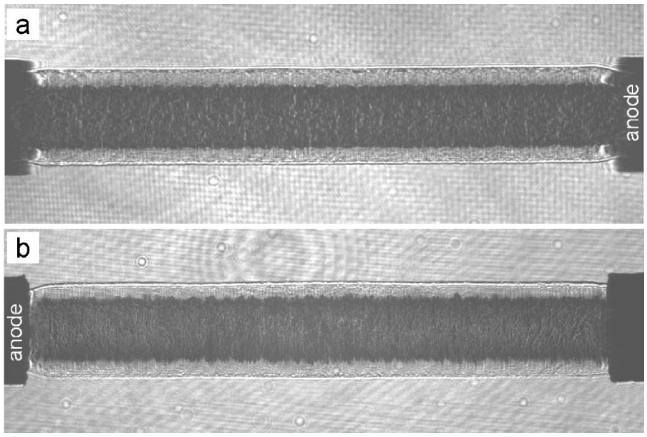

FIG. 4. Laser shadowgrams at 1 μs after voltage maximum for an air-exploded 20-μm Ti wire using a positive (a) and negative (b) polarity pulse.

cathode-anode electric field is 34 kV/cm for plus and 24 kV/cm for the minus polarity. Electrical measurements give a maximum power of 61 MW for plus and 45 MW for the minus polarity [Fig. 3(c)]. The average value of deposited energy was 5.9 eV/atom for plus and 3.4 eV/atom for minus [Fig. 3(c)]. The power of the first peak of the light emission, which is related to vapor ionization, was 450 W for positive polarity and 140 W for negative. The long-time behavior of the light emission is presented in Fig. 3(d). The positive-polarity explosion demonstrates slow increasing of radiation in 300 ns up to 550 W against of 100 W for negative one. This secondary radiation related with expanding hot microparticles and will be discussed in detail in our next paper.

The structure of deposited energy for explosions in air at 1 atm pressure is identical for positive- and negative-polarity cases. Laser shadowgrams at 1 μs after the voltage maximum for a fast-exploding 20-μm Ti wire using positive- and negative-polarity pulses are presented in Figs. 4(a) and 4(b). In both cases the wires explode absolutely homogeneously along the axis. Electrical measurements show similarities between these two explosions. The maximum power was 47 MW for plus and 44 MW for minus. The maximum cathode-anode electric field was 36 kV/cm for plus and 35 kV/cm for minus. The deposited energy up to the maximum voltage was 7.5 eV/atom for plus and 8.1 eV/atom for minus. It is interesting to point out one important feature of the fast-exploding experiments in air. In this regime no shunting breakdown occurs, as it does in the vacuum explosion. The wire expands homogeneously without separation onto a low-density/low-resistive plasma shell and a high-density/high-resistive cold core. This is a very useful explosion regime for the investigation of the metal resistivity.

Figure 5 demonstrates polarity effect for 20 μm Al wires. The conical energy deposition for positive polarity explosion on Fig. 5(a) is not as strong as for Ti wire on Fig. 2(a) but still observable. As for Ti wire, the energy deposition for Al is increasing to the anode. For negative polarity explosion [Fig. 5(b)] we see enhanced energy deposition under anode and cathode and relatively poor deposition at the central part

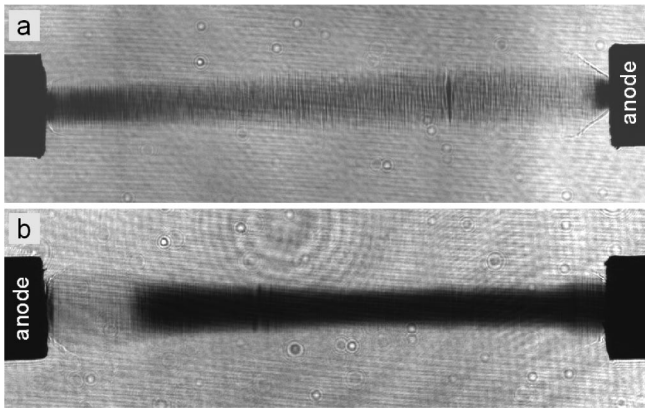

FIG. 5. Shadowgrams of exploding 20 μm Al wires for positive polarity (a) at moment 190 ns and for negative polarity (b) at moment 290 ns after voltage maximum.

of the wire as in Fig. 2(b). This effect is also not as strong as for Ti but still visible. The energy deposition before breakdown for positive explosion is $\sim$7.2 eV/atom, for negative explosion it is $\sim$5.4 eV/atom. The maximum cathode-anode electric field is 29 kV/cm for positive polarity and 20 kV/cm for negative. The power of the first peak of the light emission was 780 W for positive polarity and 380 W for negative. The maximum of electrical power is 60 MW for the plus and 56 MW for the minus polarity.

We observe the polarity effect for the fast explosion in vacuum for all nine metals tested in our experiments (Ag, Al, Cu, Au, Ni, Ti, Pt, Mo, W). The ratio of total deposited energy for positive and negative explosions vs atomization enthalpy of tested metals is presented in Fig. 6. All wires had the same 20 μm diameter and 20 mm length. Substances with higher enthalpy of atomization demonstrate a larger difference in absorbed energies before surface breakdown. The biggest difference we observe is for Ti wire, which has the highest resistivity among tested metals.

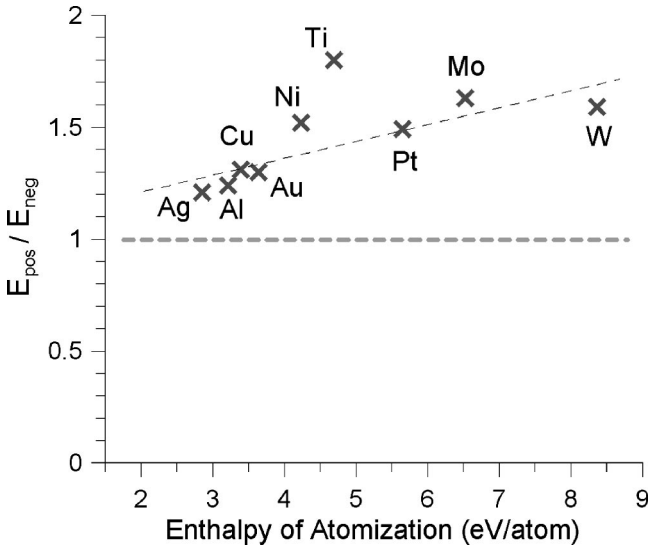

FIG. 6. Ratio of deposited energy for positive and negative polarity explosions vs atomization enthalpy for different substances.

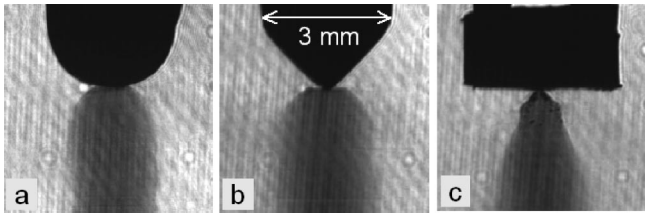

FIG. 7. Typical shadowgrams of the under-anode part of the extending $20\,\mu$m W wires at $1\,\mu$s after voltage maximum for positive polarity explosion and for three different shapes of the anode wire holder head: spherical (a), cone (b) and planar (c).

Increasing the wire diameter results in decreasing the effect of axial inhomogeneity of energy deposition for all substances and explosion modes. But in any case energy deposition for positive-polarity explosions is higher than for negative ones.

Figure 7 demonstrates shadowgrams of the under-anode part of the extending $20\,\mu$m W wires at $1\,\mu$s after voltage maximum for three different shapes of the wire holder for positive polarity explosion. It is obvious that the shape of the high-potential wire holder influences the axial structure of wire expansion.

In our experiments, we can neglect by radial inhomogeneity of the current due to skin effect because of the small wire diameter. Before surface-breakdown current flow through the wire and deposition of the Joule energy is homogeneous along the wire length. All axial inhomogeneity in energy deposition appears during the surface-breakdown phase. Our experimental data gives evidence for the direct influence of the radial electric field on the value and structure of the energy deposition.

Now we will proceed to estimate the radial electric field and the value of the electric current carried by the electron beam. In accordance with Gauss theorem, the radial electric field in the vicinity of the fine wire is proportional to $1/r$, where r is the radius. For a radial electric field we may write $E_r = 2q(z)/r$, where $q(z)$ is the electric charge of the wire per unit length. Integrating E_r over r we obtain $U \approx 2q(z)\ln(R_{\rm ex}/r_w)$, where U is the cathode-anode voltage, $R_{\rm ex}$ is the radius of the external return current cap, and r_w is the radius of the wire. Thus we may write

$$E_r(r_w,z) = k\varphi(z)\cdot U/[r_w\cdot\ln(R_{\rm ex}/r_w)], \qquad (1)$$

where $k\varphi(z)$ is the form factor of chamber geometry, with $\varphi(z)$being normalized so that $\max\{\varphi(z)\}=1$. The coefficient k should be on the order of 1. The factor $k\varphi(z)$ can be obtained by numerical simulation of the electrostatic field in the coaxial target unit. We use here $k=1$ to estimate the order of magnitude of the E_r. For our experimental geometry ($R_{\rm ex}=3.4$ cm, $l_z=2$ cm) with a 20-μm-diameter wire and with a 50-kV anode-cathode resistive voltage the axial electric field $E_z = U/l_z$ is of 3×10^4 V/cm and the radial field E_r is of order 10^7 V/cm. Thus the axial electric field in wire vicinity is of about 0.1% of the radial field. The estimated value of E_r significantly exceeds the threshold for field emission (10^5–10^6 V/cm).

For a positive-polarity explosion, the radial electric field E_r will create an external potential barrier for electronic emission from the wire surface. This potential barrier has a maximum value at the anode and drops linearly to almost zero at the cathode. With these conditions, a hot wire starts thermoelectric emission at the cathode. The emitted electrons start ionization of the ambient vapor, which causes switching of the current from the wire to the plasma shell. The ionization shunting propagates as an electron-avalanche wave into the surrounding vapor in the direction of the anode with a velocity $\sim 3\times10^8$ cm/s. In this case we observe a conical structure of the wire expansion [Fig. 2(a)] due to the increase in the energy deposition in the direction of the anode. The value of the deposited energy at the anode for refractory metals may be several times greater than at the cathode. The high-voltage anode wire holder introduces disturbance in value of radial electric field. In this case the structure of the external potential barrier near the anode will depend on the geometry of the wire holder, as in Fig. 7.

For negative-polarity explosions, the radial electric field decreases the potential barrier for electrons at the metal-vacuum interface, which stimulates earlier surface breakdown than in the positive case. The electrons emitted by the hot wire surface move mainly under action of the radial electric $2q/r$ and azimuthal magnetic $2I/cr$ fields. For a sufficiently high voltage, the radial amplitude of the cyclotron motion $r_{\rm max}$ of the emitted electron may be larger than radius of the wire r_w. In this case ''magnetic insulation'' does not prevent surface breakdown and rejection of all current from the wire to the plasma shell. The value of cyclotron motion $r_{\rm max}$ can be easily obtained by analytically using conservation of axial momentum and total electron energy:

$$\begin{aligned} r_{\rm max} &= r_w \exp(2a) \\ &\equiv r_w \exp\left(-\frac{qmc^4}{eI^2}\right) \\ &\cong r_w \exp\left(-(Zc)^2\frac{m_e c^2}{eU}\,\frac{\varphi(z)}{2\ln(R_{\rm ex}/r_w)}\right), \end{aligned} \qquad (2)$$

where Z is the electrical resistance of the wire. The formula (2) is relevant for $U<0$ only, with $a>0$. In the practical units we have $a = Z(\Omega)/[7I({\rm kA})\ln(R_{\rm ex}/r_w)]$. Thus for the 20-$\mu$m-diameter Ti wire, we have $a\approx0.96$ just before the moment of expansion at the negative polarity and $r_{\rm max} \approx 7r_w$.

When the temperature of the wire surface becomes sufficiently high to support an appropriate rate of electron emission, the cloud of emitted electrons becomes dense enough to screen the wire surface from the radial electric field. This effect leads to saturation of the electric current, which can be transported by the beam of emitted electrons. Estimates of maximum electron density and saturated electric current $I_{\rm sat}$ in vacuum surrounding the wire show that $I_{\rm sat}/I \sim (cq/I)^2 \cong \{\varphi(z)cZ/[2\ln(R_{\rm ex}/r_w)]\}^2$. For our experimental conditions the $I_{\rm sat}/I$ is of 1–2%. This current can lead to deposition of about 1–2% of the total energy into a thin ($\sim10^{-3}$ μm) surface layer and hence to early initiation of

extensive ion emission from the wire surface. Thereafter, the saturated electron beam current grows because ions compensate the space charge of the electron beam. This self-amplifying process can result in breakdown along the wire surface. Also the electron beam can start ionizing the metal vapor surrounding the hot wire. The electron beam picks up energy for ionization owing to their motion in electric field and in particular owing to their drift to anode. Thus for a negative-polarity explosion the thermofield electron emission may provoke earlier breakdown along the wire surface. This results in a smaller energy deposition for negative-polarity explosions than for positive ones. It is very important that the radial electric field that expels the electrons from the wire for the negative polarity should be suppressed near the massive high-conductivity electrodes because of their screening action. Hence the intensity of the electron beam should be suppressed near the electrodes and should lead to enhanced energy deposition before surface breakdown (Figs. 2(c) and 2(d)).

For explosions in air (Fig. 5) the emitted electrons cannot ionize the surrounding gas because of its high density ($\sim 10^{19}$ cm^{-3}). For this case a shunting, low-resistance plasma shell is absent and wires explode homogeneously along the length. The wire starts expanding because the internal gas kinetic pressure exceeds the pressure of the magnetic field.

It is well known that refractory metals are more powerful electronic emitters than nonrefractory. This is the reason why polarity effect is stronger for refractory metals (Fig. 2) and weaker for nonrefractory (Fig. 5).

According to formula (2) the parameter a is proportional to Z and r_w^{-2}. The saturated current of electron beam I_{sat}/I is proportional to Z^2 *and* r_w^{-4}. This means that the degree to which the magnetic insulation overcomes the saturated beam current depends strongly on diameter of the wire. Thus, the polarity effect should be much weaker for wires with larger diameters, as seen in the experiment.

To make a reasonable estimate of the electric field structure in the wire vicinity the computer electrostatic simulation has been done taking into account experimental geometry of the coaxial target unit in Fig. 1. A 2D electrostatic code, that is a modified version of the code described in Ref. [10], is used. Why can we use electrostatic simulation for estimation of the electric field structure in ns time-scale explosions? The typical size of electrodes, which surround wire, is about 3 cm and time of flight for light between electrodes equals $\Delta t = 0.1$ns. The quasistationary field distribution will take place in the system after certain Δt, which is roughly 1 ns. The duration of the quasistationary process is determined by the inductance of cavity with wire (~ 50 nH) and sum of wire resistance ($1-100\ \Omega$) and wave resistance of cable ($50\ \Omega$). This value is about 0.5–1 ns. Both of these evaluations are about 1 ns. Because the typical rise time for current and voltage before the surface breakdown is 10–15 ns, we can conclude that electrostatic simulation for electric field is correct enough for our processes. Taking into account the wave or/and quasistationary processes will increase the value of radial electric field.

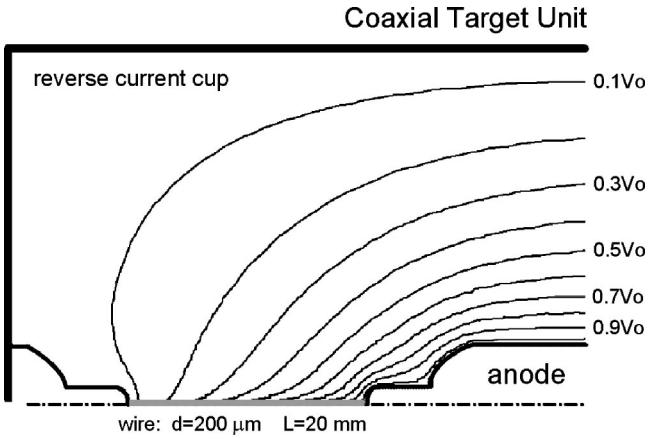

FIG. 8. The structures of equipotential lines of electric field simulated for coaxial target unit geometry on Fig. 1. The cathode-anode voltage was V_0.

The simulation has been performed for resistive wire with $200\ \mu$m diameter and 2 cm length. The large wire diameter was used to avoid an enormously tight numerical grid to achieve reasonable accuracy of the simulation. Figure 8 presents the axially symmetric equipotential surfaces of electric field for the positive polarity explosion. The symmetry axis is shown in Fig. 8 by the dashed-dotted line. We can see that equipotential lines become concentrated under the anode, which causes growth of the radial electric field in that area.

At the cathode the radial field can even change its direction. Figure 9 presents the distribution of the radial electric field along the $20\,\mu$m wire surface. Far from the wire holders the radial field increases almost linearly from the cathode to the anode. Radial electric field in a wire vicinity can be approximated by the formula (1) assuming that r_w- is radius, $k \approx 0.53$ and with $\varphi(z)$ normalized form factor. The radial

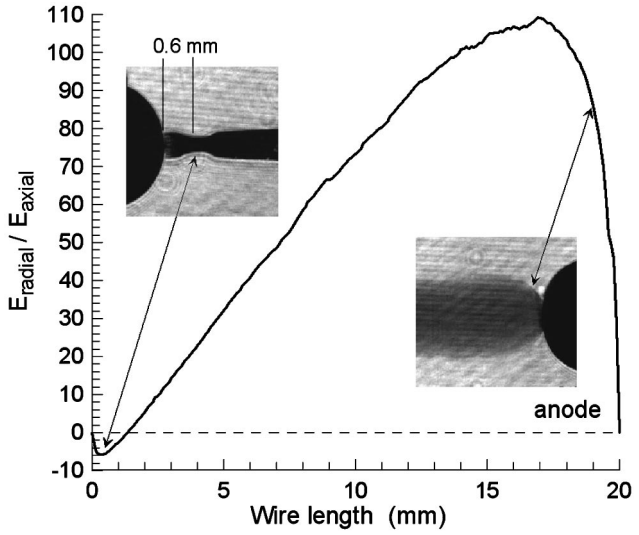

FIG. 9. Distribution of the relative radial electric field along the 20 μm wire surface. The axial field is a constant and equals V_0/L. Arrows shows features on shadowgram of expanding 20 μm W wire at 1 μs, which is corresponding to ''edge effects'' feature in radial electric field structure.

field starts to drop after 3 mm from the high-potential anode. The fragment of the shadowgram of exploding 20 μm W wire on Fig. 9 demonstrates the same under-anode feature. The higher the value of the radial field the stronger the wire overheating. A more remarkable observation can be made at the low-potential cathode. The position of the minimum of the radial electric field does not coincide with the cathode but is displaced to the anode ~ 0.5 mm. In that region the radial electric field has a sign other than that for the rest of the wire. In this case the electronic emission and vapor breakdown should start from the position of the local minimum field. Exactly the same situation can be observed at the low-potential cathode part for exploding W wire in Fig. 9. The minimum wire expansion is displaced 0.6 mm from the cathode, which means that shunting breakdown starts first at that position. Thus, we can see that behavior of the radial field determines the axial structure of wire overheating.

For negative polarity explosion the high radial electric field accelerates electronic emission from the wire surface due to lowering of the potential barrier. The region with a smaller field becomes more overheated than the region with a higher field. Such peculiarities of radial field distribution along the wire result in weak energy deposition at the central part of the wire and enhanced at the cathode and anode, as in Figs. 2(c) and 2(d).

We can see from Fig. 9 that the low-field region is more extended under the low-potential wire holder than under the high potential. It explains the asymmetry in energy deposition on Figs. 2(c) and 2(d) for the low-potential anode and the high-potential cathode.

It is obvious that the shape of the wire holders plays an important role in the topology of disturbance of the electric field. These different ''edge effects'' give different overheating on exploding wires, as we see in Fig. 7. We will skip this analysis in our paper because it is too obvious.

In conclusion, we reveal a strong influence of the radial electric field on the value and structure of the deposited energy into thin metal wires during their fast electrical explosion into vacuum. This effect can be explained by the influence of electron emission in forming a plasma shell, generating an electron beam along the wire, and axial propagation of a breakdown-shunting wave. The ''polarity effect'' allows better understanding and control of processes leading to creation of a plasma shell and its symmetry, which is very important for modern multiwire array *Z*-pinch experiments.

The authors gratefully acknowledge H. Faretto, A. Oxner, and A. Astanovitskiy for technical assistance. Special thanks go to E. Grabovski for useful discussions. The project has been supported partially by DOE-NV, DOE-EPSCoR, SNI (Contract No. AX-2863), UNR, Cornell University (contract 1980524), and in part by the RFBR (Grant No. 01-02-17526). Sandia is a multiprogram laboratory operated by Sandia Corporation, a Lockheed Martin Company, for the United States Department of Energy under Contract No. DE-AC04-94AL8500.

[1] T. W. Sanford *et al.*, Phys. Rev. Lett. **77**, 5063 (1996).
[2] R. B. Spielman *et al.*, Phys. Plasmas **5**, 2105 (1998).
[3] F. N. Beg *et al.*, Phys. Plasmas **9**, 375 (2002).
[4] F. D. Bennett, *High Temperature Exploding Wire*, in *Progress in High Temperature Physics and Chemistry*, edited by C. A. Rouse (Pergamon Press, Oxford, 1968), Vol. 2, pp. 1-63.
[5] S. V. Lebedev and A. I. Savvatimskii, Uspekhi Fiz. Nauk **144**, 215 (1984) (in Russian) [Sov. Phys. Usp. **27**, 749 (1984)].
[6] A. V. Branitskii *et al.*, in *Proceedings of 12th International Conference on High-Power Particle Beams (BEAMS'98), Haifa, Israel, 1998*, edited by M. Makkovits and J. Shilon (Haifa, Rafael, 1998), Vol. 2, p. 599.
[7] D. B. Sinars *et al.*, Phys. Plasmas **7**, 429 (2000).
[8] V. S. Sedoi *et al.*, IEEE Trans. Plasma Sci. **27**, 845 (1999).
[9] G. S. Sarkisov, B.S. Bauer, and J.S. De-Groot, Pis'ma Zh. Eksp. Teor. Phyz., 73, 74 (2001) [JETP Lett. **73**, 69 (2001)].
[10] N.K. Gorbenko, V.P. Iljin, G.S. Popova, and A.M. Sveshnikov. Codes package EHRA for electrostatic simulations, in *Numerical Methods of Solving of Electron Optics Problems* (Siberian Division of USSR AS, Novosibirsk, 1979) (in Russian).